RCCI 연소의 직접수치모사 연구 - 화학적 측면

Minh Bau Luong* · 유광현* · 유춘상*†

A DNS Study of RCCI Combustion - Chemical Aspects

Minh Bau Luong*, Gwang Hyeon Yu*, Chun Sang Yoo*†

ABSTRACT

The chemical aspects of primary reference fuel (PRF)/air mixture under RCCI conditions are investigated to provide fundamental insights into the ignition characteristics of RCCI combustion. Chemical explosive mode analysis (CEMA) is adopted to understand the ignition process of the lean PRF/air mixture by identifying controlling species and elementary reactions at different locations and times.

Key Words: DNS, HCCI, RCCI, chemical explosive mode analysis (CEMA)

In this study, the chemical aspects of reactivity controlled compression ignition (RCCI) combustion are investigated by analyzing two-dimensional direct numerical simulation (2-D DNS) data with the chemical explosive mode (CEM) analysis. The DNSs were performed with a 116-species reduced mechanism of primary reference fuel (PRF). RCCI combustion uses two fuels with different reactivity. For example, *n*-heptane (n-C_7H_{16}) and i*so*-octane (i-C_8H_{18}) can be used because they are representative of highly reactive and less reactive fuels, respectively. The overall low-temperature (LT), intermediate-temperature (IT), and high-temperature (HT) reaction pathways of *n*-heptane and *iso*-octane oxidation relevant to RCCI combustion are shown in Fig. 1he details of the pathways can be found in [1-2].

The initial conditions of mean pressure, mean temperature, mean equivalence ratio, and mean global PRF number for 2-D DNS are p_0 = 40 atm, T_0 = 900 K, and ϕ_0 = 0.45, and PRF50, respectively. Fig. 2 shows the temporal evolutions of the mean heat release rate (HRR) and the mean fractions of important species for 2-D DNS, which exhibit a staged consumption of more reactive fuel, *n*-heptane, and less reactive fuel, *iso*-octane. *n*-Heptane is primarily consumed during the first-stage ignition, following the LT reaction pathway in

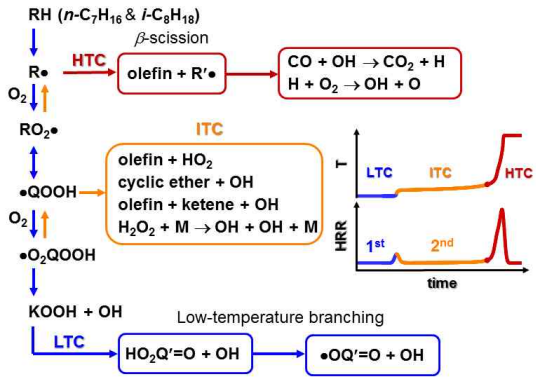

Fig. 1 Schematic of reaction pathways

Fig. 1. Then, the remaining *n*-heptane and most *iso*-octane are consumed by the IT and HT reaction pathways. During these stages, *n*-heptane and *iso*-octane are decomposed into HO_2, CH_2O, C_2H_4, and other smaller molecules. Consumption of CH_2O, decomposition of H_2O_2, and production of OH appear to coincide with the consumption of all remaining *iso*-octane, followed by the oxidation of CO into CO_2.

It is believed that local mixtures with high *n*-heptane concentration (e.g.~ PRF30 in the present study - a mixture of 30% i*so*-octane and 70% *n*-heptane by volume) auto-ignite first and then initiate adjacent less-reactive mixtures, resulting in a sequential ignition process. Therefore, the CEM analysis is first applied to the 0-D ignition of PRF30/air mixture under conditions of p_0 = 40 atm, T_0 = 812 K, and ϕ_0 = 0.74 (high *n*-heptane concentration with low T due to evaporative

* 유니스트 기계공학과
† 연락저자, csyoo@unist.ac.kr
TEL : (052)217-2322 FAX : (052)217-2409

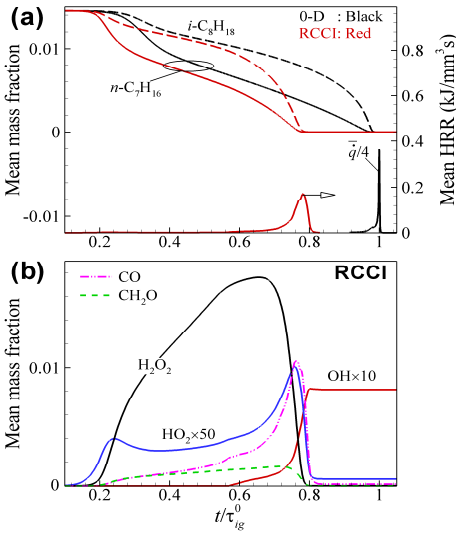

Fig. 2 Temporal evolutions of the mean HRR and mean mass fractions of important species. The 0-D ignition is also added for comparison.

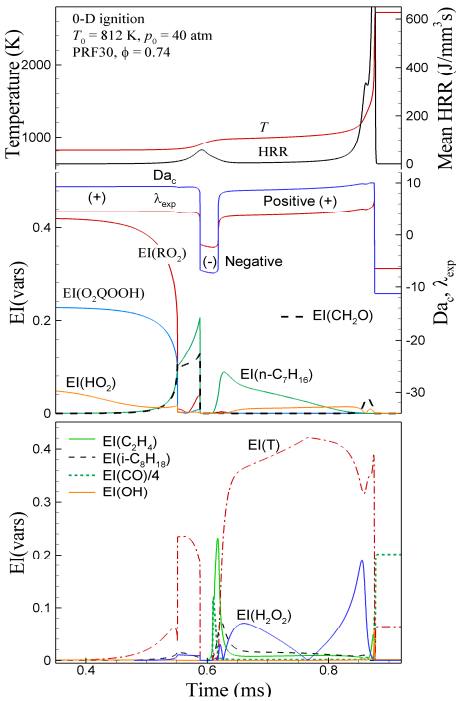

Fig. 3 Temporal evolutions of temperature, HRR, Da_c, $\lambda_{exp} \equiv \text{sign}(\text{Re}(\lambda e)) \times \log(1+|\text{Re}(\lambda e)|)$, EI of important species for 0-D ignition

cooling effect) as shown in Figs. 3 and 4. Readers are referred to [3-4] for the details of the CEMA formulation and the application of the CEMA can be found in [5-8]. Note that

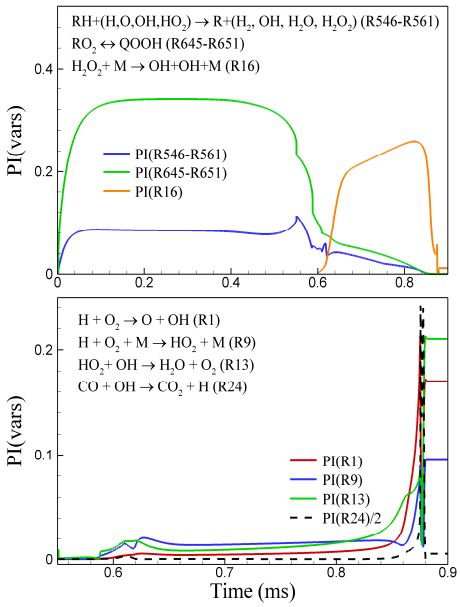

Fig. 4 Temporal evolutions of PI of important reactions for 0-D ignition

(1) a mixture with a negative $\text{Re}(\lambda_e)$ is already burned while the ignition of mixture with a positive $\text{Re}(\lambda_e)$ is still underway; (2) important species and reactions are identified by relative magnitudes of EI and PI values, respectively. As shown in Fig. 3 and Fig. 4, during the early stage of combustion, RO_2, O_2QOOH, and HO2 are controlling species, and

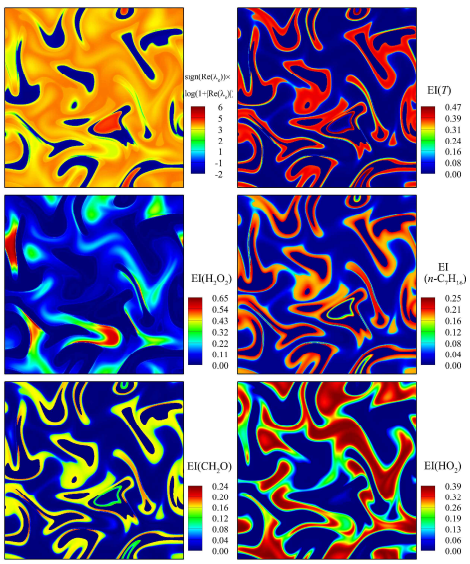

Fig. 5 Isocontours of $\text{sign}(\text{Re}(\lambda e)) \times \log(1+|\text{Re}(\lambda e)|)$, and EI of important species at the first-stage ignition.

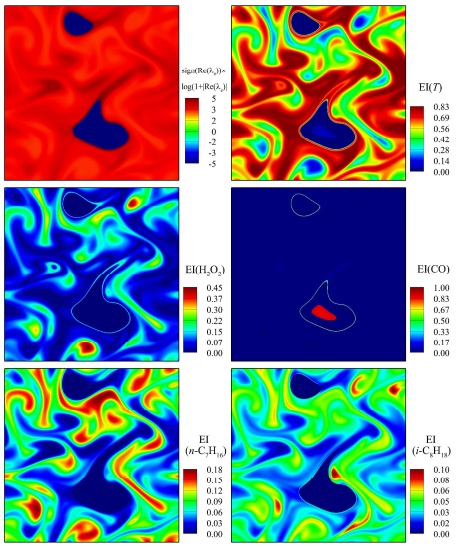

Fig. 6 Isocontours of sign(Re(λe))×log(1+|Re(λe|)), and EI of important species at 15% cumulative heat release rate (CHRR).

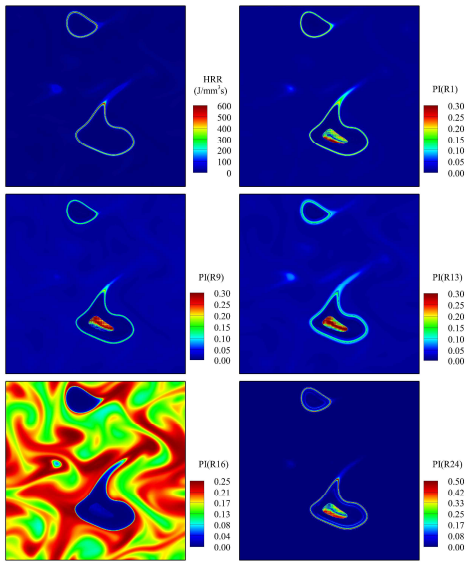

Fig. 7 Isocontours of HRR, and PI of important reactions at starting of the main combustion.

R + (H, O, OH, HO_2) → R + (H_2, OH, H_2O, H_2O_2), and RO_2 → QOOH are controlling reactions. However, during the first-stage ignition, n-C_7H_{16} and CH_2O become the most important species. Right after the first-stage ignition, H_2O_2 + M → OH + OH + M (R16) becomes active, and temperature becomes the most important factor governing the

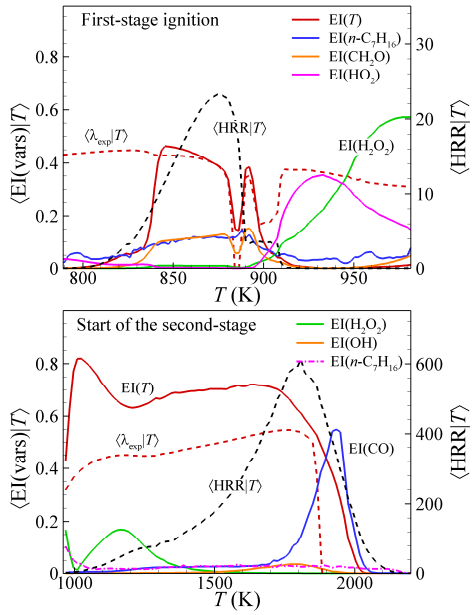

Fig. 8 The conditional mean of HRR and EI of controlling species on temperature at (a) the first-stage ignition, and at (b) the 15% CHRR

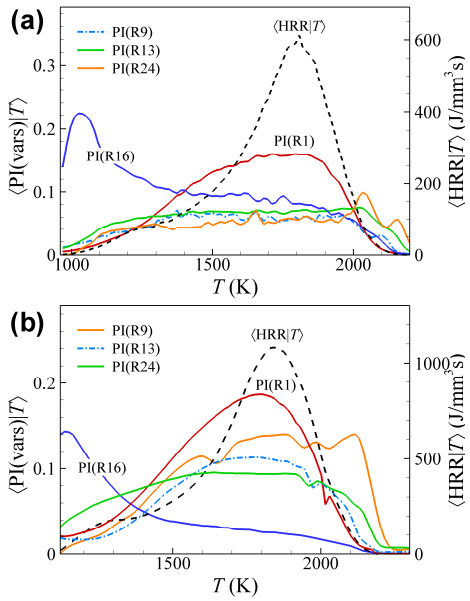

Fig. 9 The conditional mean of HRR and PI of controlling reactions on temperature at (a) the 15% CHRR, and at (b) the second-stage ignition

combustion process compared to the contributions of n-C_7H_{16}, i-C_8H_{18}, and H_2O_2. At the main combustion event, together with

temperature, H_2O_2, OH, and CO become controlling variables, and H + O_2 → O + OH (R1) and CO + OH → CO_2 + H (R24) are controlling reactions.

Next, the same EI and PI analyses are applied to the 2-D DNS and the contours of EI and PI of critical species and reactions at different locations and time are shown in Figs. 5-7. The corresponding conditional means on temperature are calculated and shown in Fig. 8 for <EI(vars)|T> and Fig. 9 for <PI(vars)|T>. The 2-D CEM results are consistent with the findings from the 0-D ignition discussed above. However, it further reveals that at the low temperature regions (T < 900 K), temperature, CH_2O and n-C_7H_{16} are the key variables, while at the intermediate temperature regions (900 K < T < 1000 K), HO_2 and H_2O_2 become the most critical species as readily seen in Fig. 8. Moreover, as shown in Fig. 9, at T ~ 1000-1200 K, the chain-branching reaction of H_2O_2 via H_2O_2 + M → OH + OH + M (R16) becomes highly reactive, which subsequently results in initiating high temperature chemistry. Moreover, heat is primarily released at the locations of very thin flame-like fronts (deflagrations) via the reaction CO + OH → CO_2 + H (R24), which is triggered by the chain branching reaction, H + O_2 → O + OH (R1) as readily observed in Figs. 7 and 9.

The chemical aspects of the ignition process of PRF/air mixture under RCCI conditions were investigated by using CEM analysis. low temperature, CH_2O and n-C_7H_{16} are identified as the predominant factors contributed to the CEM at the first-stage ignition, while the chain branching reaction of H_2O_2 and the production reaction of HO_2 are the main reactions of the IT combustion. During thermal ignition, however, temperature is found to be the predominant factor and high-temperature reactions represented by H + O_2 → O + OH are responsible for the thermal ignition. At deflagrations, temperature, CO, and OH are the most important species while the conversion reaction of CO to CO_2 and high-temperature chain branching reaction of H + O_2 → O + OH are identified to be important to the CEM.

Acknowledgements

This research was supported by Basic Science Research Program through the National Research Foundation of Korea (NRF) funded by the Ministry of Science, ICT & Future Planning (No. 2015R1A2A2A01007378) and the 2015 Research Fund (1.150033.01) of UNIST. This research used the resources of the KAUST Supercomputing Laboratory.

References

[1] M.B. Luong, Z. Luo, T. Lu, S.H. Chung, C.S. Yoo, Combustion and Flame 160 (2013) 2038 - 2047.
[2] M.B. Luong, G.H. Yu, T. Lu, S.H. Chung, C.S. Yoo, Combustion and Flame 162 (2015) 4566-4585.
[4] Z. Luo, C.S. Yoo, E.S. Richardson, J.H. Chen, C.K. Law, T. Lu, Combust. Flame, 159 (2012) 265-274
[5] R. Shan, C.S. Yoo, J.H. Chen, T. Lu, Combust. Flame, 159 (2012) 3119-3127.
[6] C.S. Yoo, T. Lu, J.H. Chen, and C.K. Law, Combust. Flame 158 (2011) 1727-1741.
[7] M.B. Luong, T. Lu, S.H. Chung, C.S. Yoo, Combust. Flame 161 (2014) 2878-2889.
[8] S.O. Kim, M.B. Luong, J.H. Chen, C.S. Yoo, Combust. Flame 162 (2015) 717-726.